Electronic Supplementary Material (ESI) for New Journal of Chemistry.
This journal is © The Royal Society of Chemistry and the Centre National de la Recherche Scientifique 2015

*Electronic Supplementary Information for:*

# Towards a Potential 4,4'-(1,2,4,5-Tetrazine-3,6-diyl) Dibenzoic Spacer to Construct Metal-Organic Frameworks

Antonio J. Calahorro,[a] Belén Fernández,[a] Celeste García-Gallarín,[b] Manuel Melguizo,[b] David Fairen-Jimenez[c,]* Guillermo Zaragoza,[d] Alfonso Sallinas-Castillo,[e] Santiago gómez-Ruiz[f] and Antonio Rodríguez-Diéguez.[a,]*

[a]*Departamento de Química Inorgánica, Universidad de Granada, 18071, Granada, Spain. Tel: 0034958240442; E-mail: antonio5@ugr.es*
[b]*Departamento de Química Inorgánica y Orgánica, Universidad de Jaén, Campus Las Lagunillas, 23071, Jaén, Spain.*
[c]*Dept. of Chemical Engineering & Biotechnology, University of Cambridge, United Kingdom. E-mail: df334@cam.ac.uk*
[d]*Unidad de Rayos X; RIAIDT Edificio CACTUS, Universidad de Santiago de Compostela, 15782 Santiago de Compostela, Spain.*
[e]*Departamento de Química Analítica, Universidad de Granada, 18071, Granada, Spain*
[f]*Department of Chemical and Energy Technology, Rey Juan Carlos University 28933 Móstoles, Spain.*

**Index:**



## 1. X-Ray diffraction

Suitable crystals of **1** and **2** were mounted on a glass fibre and used for data collection on a Bruker AXS APEX CCD area detector equipped with graphite monochromated Mo Kα radiation (λ = 0.71073 Å) by applying the ω-scan method. Lorentz-polarization and empirical absorption corrections were applied. The structures were solved by direct methods and refined with full-matrix least-squares calculations on $F^2$ using the program SHELXS97.[1] Anisotropic temperature factors were assigned to all atoms except for hydrogen atoms, which are riding their parent atoms with an isotropic temperature factor arbitrarily chosen as 1.2 times that of the respective parent. In general, the quality of data is very low, several crystals of **1** and **2** were measured and the structure was solved from the best data we were able to collect. Final R(F), wR($F^2$) and goodness of fit agreement factors, details on the data collection and analysis can be found in Table S1. Selected bond lengths and angles are given in Tables S2 and S3. CCDC reference numbers for the structures were 1030582-1030583. Copies of the data can be obtained free of charge upon application to CCDC, 12 Union Road, Cambridge CB2 1EZ, U.K. (fax, (+44)1223 336-033; e-mail, deposit@ ccdc.cam.ac.uk).

**Table S1.** Selected Distances (Å) for compound **1**, **2** and **3**

| **1** | **2** |
|---|---|
| O1 C1 1.332(11) | K1 O2 2.693(2) |
| O1 H1O 0.92(9) | K1 O2 2.693(2) |
| O2 C1 1.235(11) | K1 O1 2.842(2) |
| C1 C2 1.452(13) | K1 O1 2.843(2) |
| C2 C3 1.384(12) | K1 O2 2.885(2) |
| C2 C7 1.418(13) | K1 O2 2.885(2) |
| C3 C4 1.395(12) | K1 O1 3.163(2) |
| C4 C5 1.418(12) | K1 O1 3.163(2) |
| C5 C6 1.402(12) | K1 H1O 2.97(8) |
| C5 C8 1.446(12) | |
| C6 C7 1.376(12) | |
| C8 N1 1.337(11) | |
| C8 N2 1.363(11) | |
| N1 N2 1.323(9) | |
| N2 C8 1.363(11) | |
| S1 O3 1.504(6) | |
| S1 C10 1.759(9) | |
| S1 C9 1.779(10) | |

**Table S2.** Selected Bond Angles (Å) for compound **1**, **2** and **3**

| **1** | **2** |
|---|---|
| O2 C1 O1 121.6(9) | O2 K1 O2 152.12(10) |
| O2 C1 C2 124.7(10) | O2 K1 O1 69.91(6) |
| O1 C1 C2 113.7(10) | O2 K1 O1 120.45(6 |
| C3 C2 C7 116.8(9) | O2 K1 O1 120.45(6) |
| C3 C2 C1 123.3(9) | O2 K1 O1 69.91(6) |
| C7 C2 C1 119.8(8) | O1 K1 O1 140.38(10) |
| C2 C3 C4 122.7(9) | O2 K1 O2 74.24(5) |
| C3 C4 C5 119.4(9) | O2 K1 O2 84.38(7) |
| C6 C5 C4 118.5(9) | O1 K1 O2 138.58(7) |
| C6 C5 C8 121.3(9) | O1 K1 O2 76.70(6) |
| C4 C5 C8 120.2(9) | O2 K1 O2 84.38(7) |
| C7 C6 C5 120.5(9) | O2 K1 O2 74.24(5) |
| C6 C7 C2 121.9(9) | O1 K1 O2 76.70(6) |
| N1 C8 N2 122.8(9) | O1 K1 O2 138.58(7) |
| N1 C8 C5 119.4(10) | O2 K1 O2 79.84(9) |
| N2 C8 C5 117.7(10) | O2 K1 O1 124.23(7) |
| N2 N1 C8 119.4(8) | O2 K1 O1 83.17(6) |
| N1 N2 C8 117.8(7) | O1 K1 O1 72.62(5) |
| O3 S1 C10 105.5(4) | O1 K1 O1 71.01(7) |
| O3 S1 C9 106.4(5) | O2 K1 O1 147.67(6) |
| C10 S1 C9 99.4(5) | O2 K1 O1 124.60(6) |
| | O2 K1 O1 83.17(6) |
| | O2 K1 O1 124.23(7) |
| | O1 K1 O1 71.00(7) |
| | O1 K1 O1 72.62(5) |
| | O2 K1 O1 124.60(6) |
| | O2 K1 O1 147.67(6) |
| | O1 K1 O1 45.84(8) |

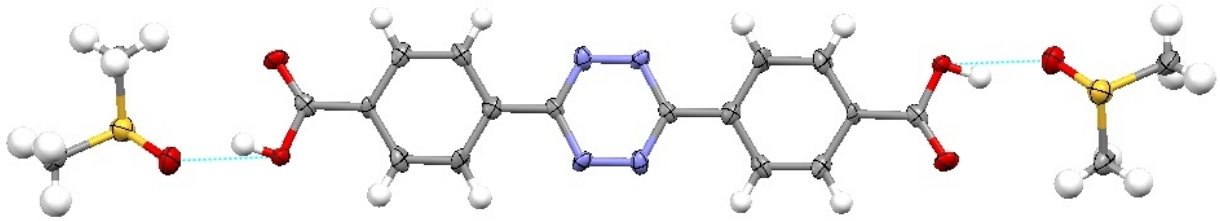

**Figure S1.** Hydrogen bonds among the terminal carboxylate groups and crystallization dimethyl-sulfoxide molecules.

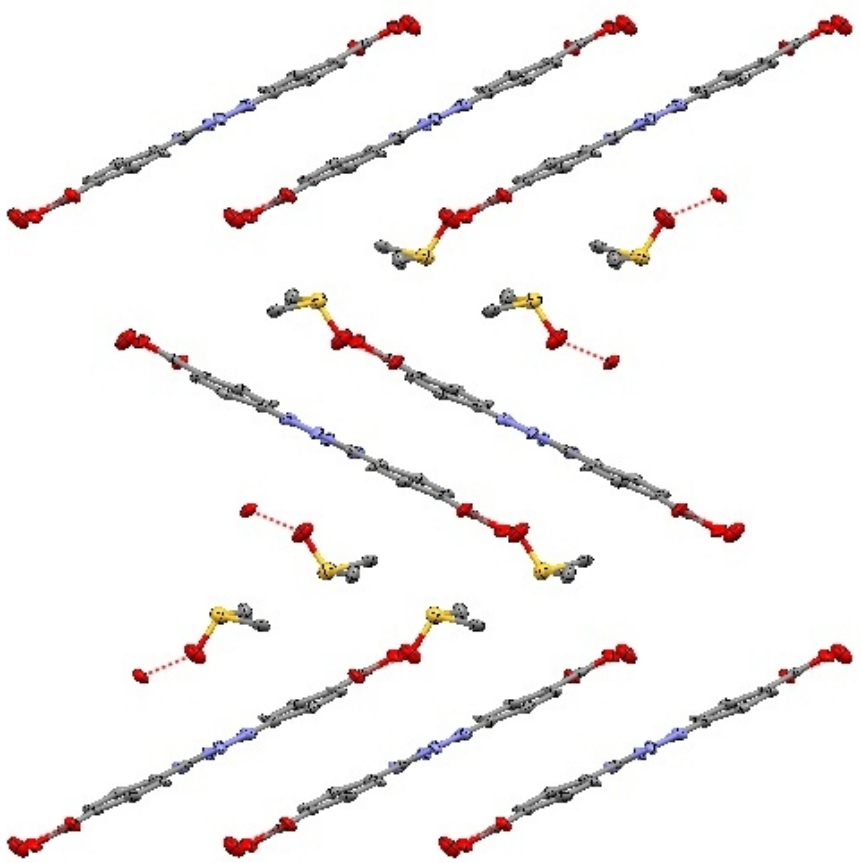

**Figure S2**. Three-nuclear units packed thought stacking interactions.

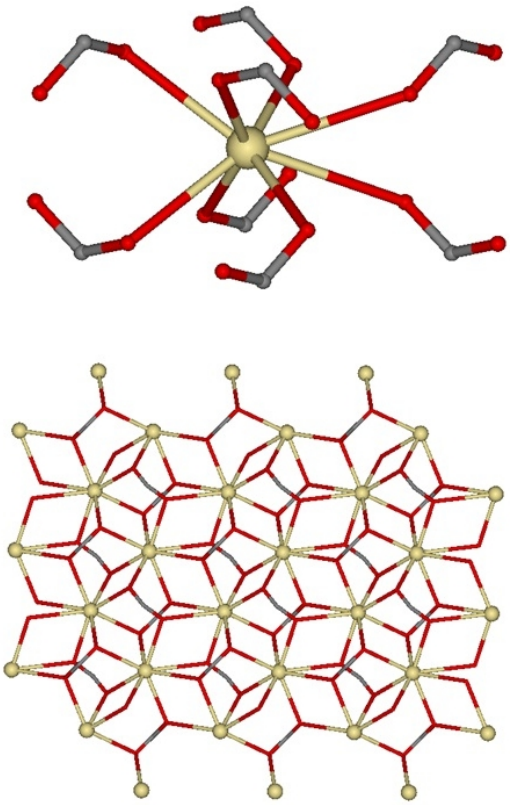

**Figure S3.** Coordination environment of potassium ions (*up*) and view down to the *a* axis in the sheet formed by potassium ions and carboxylate groups in **2** (*bottom*).

## 2. Structure Prediction

The structures of **3** and **4** were modeled using the structure of the original cubic IRMOF-16 (a = b = c = 21.4903 Å, *Im3m*) and incorporating the nitrogen atoms in the central aromatic ring of the ligand. The structure was then subject to geometry optimization, without any symmetry constrains using P1, based on molecular mechanics calculations. This procedure allows the modification of the position of all the atoms in the structure in order to minimize the energy. These calculations were performed with the Forcite module of Materials Studio, using an algorithm that is a cascade of the steepest descent, adjusted basis set Newton-Raphson, and quasi-Newton methods. The bonded and the short range (van der Waals) non-bonded interactions between the atoms were modeled using the Universal Force Field.[2] A cutoff distance of 12 Å was used for the LJ interactions during the geometry optimization. The long range, electrostatic, interactions, due to the presence of partial atomic charges, were modeled using a Coulombic term. The Ewald sum method was used to compute the electrostatic interactions. Partial atomic charges were derived from the charge equilibration method[3] (QEq) as implemented in Forcite.

## 3. Gas adsorption simulation

The adsorption of $N_2$ was investigated using grand canonical Monte Carlo (GCMC)[4] simulations implemented in RASPA.[5] We used an atomistic model for the MOF structures, in which the framework atoms were kept fixed at the crystallographic positions. We used the standard Lennard-Jones (LJ) 12-6 potential to model the interactions between the framework and the gases. Apart from the LJ, we included a Coulomb potential. The parameters for the framework atoms were obtained from the UFF force field. $N_2$ and $CO_2$ were modeled using the TraPPE potential with charges placed on each atom and at the center of mass. Partial atomic charges of the MOF were derived from the charge equilibration method (QEq). The Lorentz-Berthelot mixing rules were employed to calculate fluid-solid parameters. LJ interactions beyond 18 Å were neglected. $10^7$ Monte Carlo steps were performed, the first 50% of which were used for equilibration, and the remaining steps were used to calculate the ensemble averages. To calculate the gas-phase fugacity we used the Peng-Robinson equation of state.[6] After equilibration, density distributions were obtained by storing the center of mass positions of all the adsorbed molecules at regular intervals during the simulation. These density distributions provide valuable information about the preferential adsorption sites and the local spatial disorder of the adsorbed molecules. Snapshots represent one single molecular configuration during the simulation.

**Table S3.** Lennard-Jones parameters for framework atoms and the gas molecules.

| | σ [Å] | ε/k [K] | q [e] |
|---|---|---|---|
| Zn | 2.624 | 62.397 | |
| C | 3.431 | 52.838 | |
| N | 3.261 | 34.722 | |
| H | 2.571 | 22.142 | |
| F | 2.998 | 25.160 | |
| N_$N_2$ | 3.310 | 36.000 | -0.482 |
| N_com | 0 | 0 | 0.964 |
| C_$CO_2$ | 2.800 | 27.000 | +0.700 |
| O_$CO_2$ | 3.050 | 79.000 | -0.350 |

The pore volume, used to compute excess adsorption from the simulated absolute adsorption, was obtained using a Widom particle insertion method, by probing the structure with a helium molecule at room temperature, recording a large number of random points not overlapping the van der Waals volume of the framework.

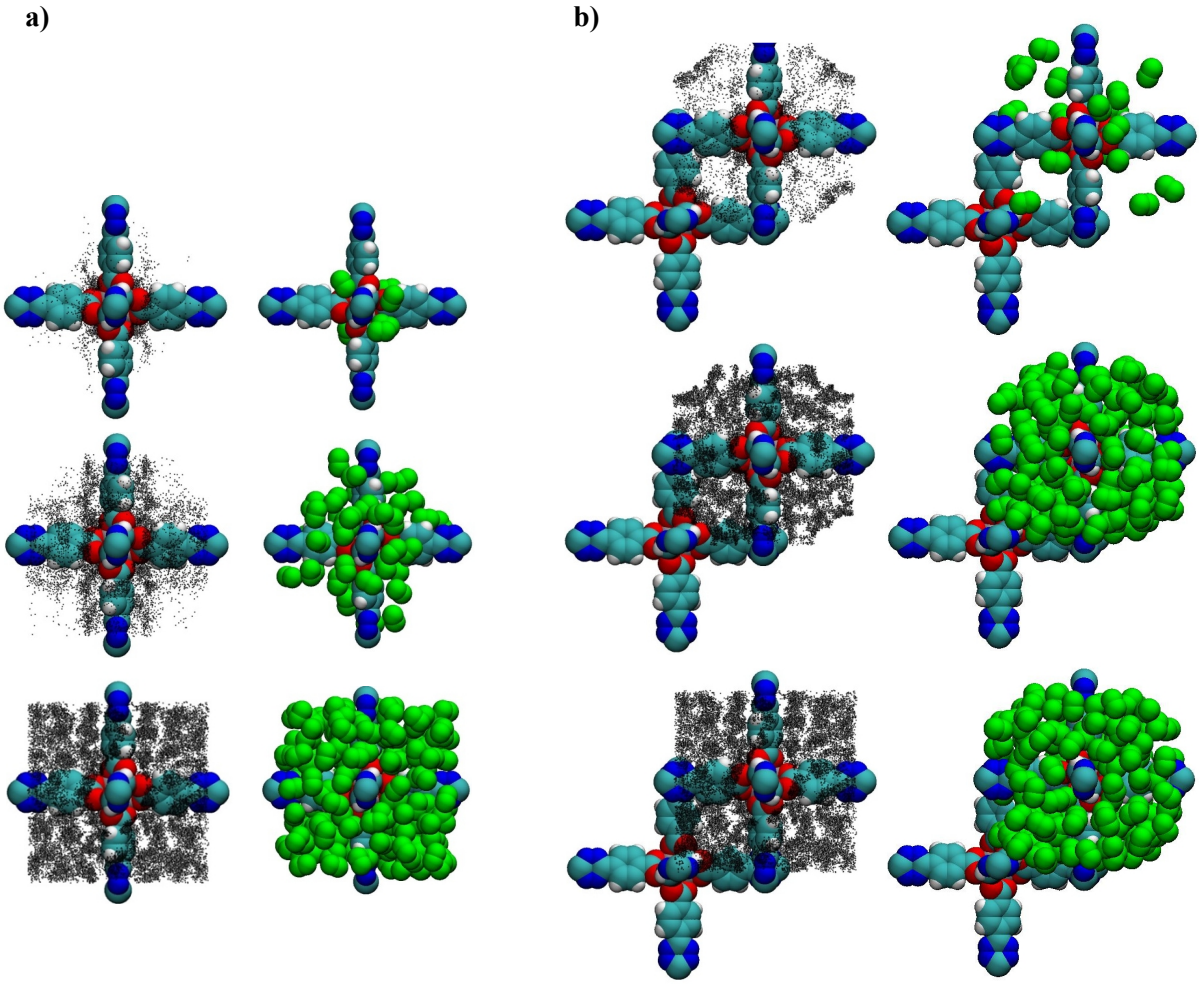


**Figure S4.** Density distributions (***left***) and snapshots (***right***) of $N_2$ adsorption at 77 K on (***a***) **3** and (***b***) **4** at low, medium and high loadings, obtained by GCMC. Black points and green spheres represent the $N_2$ molecules in the density distributions and snapshots, respectively.

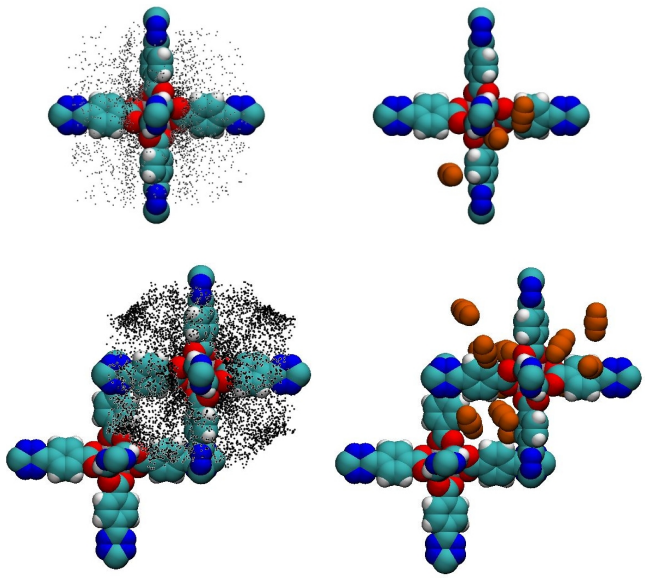

**Figure S5.** Density distributions (***left***) and snapshots (***right***) of $CO_2$ adsorption at 298 K on (***top***) **3** and (***bottom***) **4** at low loadings, obtained by GCMC. Black points and orange spheres represent the $CO_2$ molecules in the density distributions and snapshots, respectively.

## 4. RMN Studies.

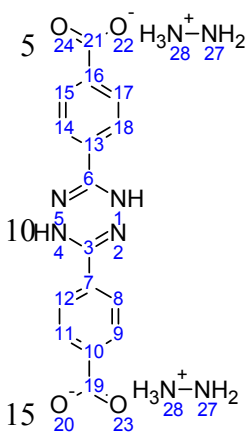

$^{1}$H NMR (400 MHz, DMSO-$d_6$) δ ppm 7.93 (4 H, d, *J*=8.70 Hz, H8/H12/H14/H18) 7.99 (4 H, d, *J*=8.50 Hz, H9/H11/H15/H17) 8.13 (10 H, br. s., hydrazonium NH) 9.29 (2 H, s, dihydrotetrazine NH).

$^{13}$C NMR (101 MHz, DMSO-$d_6$) δ ppm 126.12 (C8/C12/C14/C18), 129.40 (C9/C11/C15/C17), 132.04 (C10/C16), 133.90 (C7/C13), 147.12 (C3/C6), 166.71(carboxylates).

$^{13}$C NMR (125.7 MHz, solid state CP-MAS-TOSS) δ ppm 121.2-133.0 (phenyl carbons), 148.0 (amidine-type C3/C6),

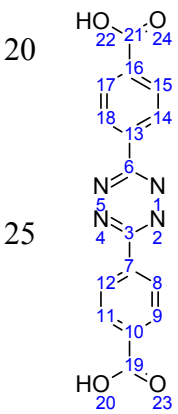

$^{13}$C NMR (125.7 MHz, solid state CP-MAS-TOSS) δ ppm 124.2-137.0 (phenylene carbons), 161.7 (tetrazine C3/C6), 171.8 (carboxyls).

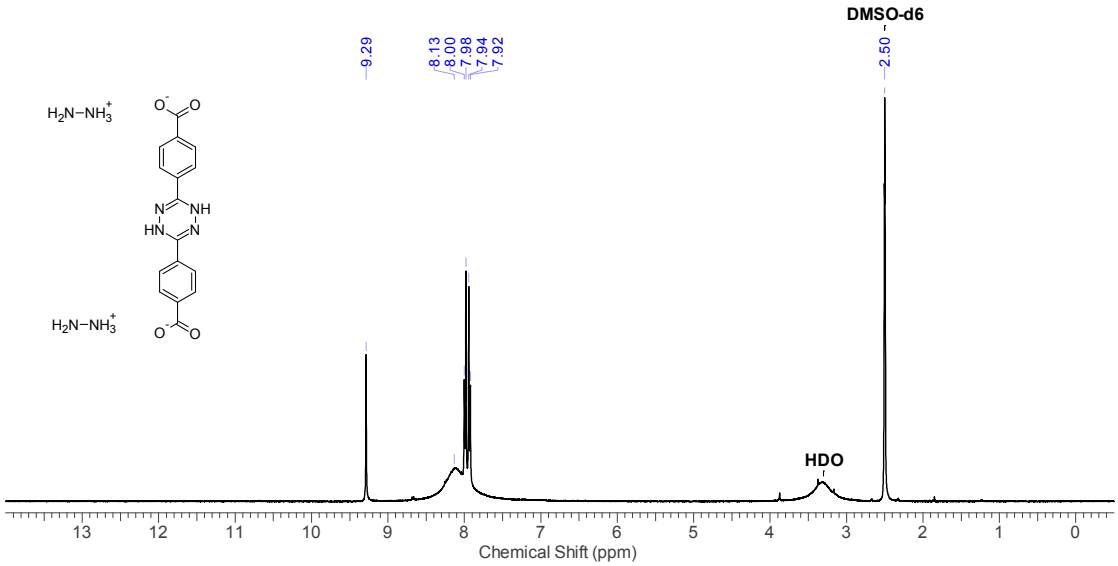


**Fig S6.** 1H NMR (400 MHz, DMSO-d6) of 4,4'-(1,2,4,5-tetrazine-3,6-diyl)dibenzoic.

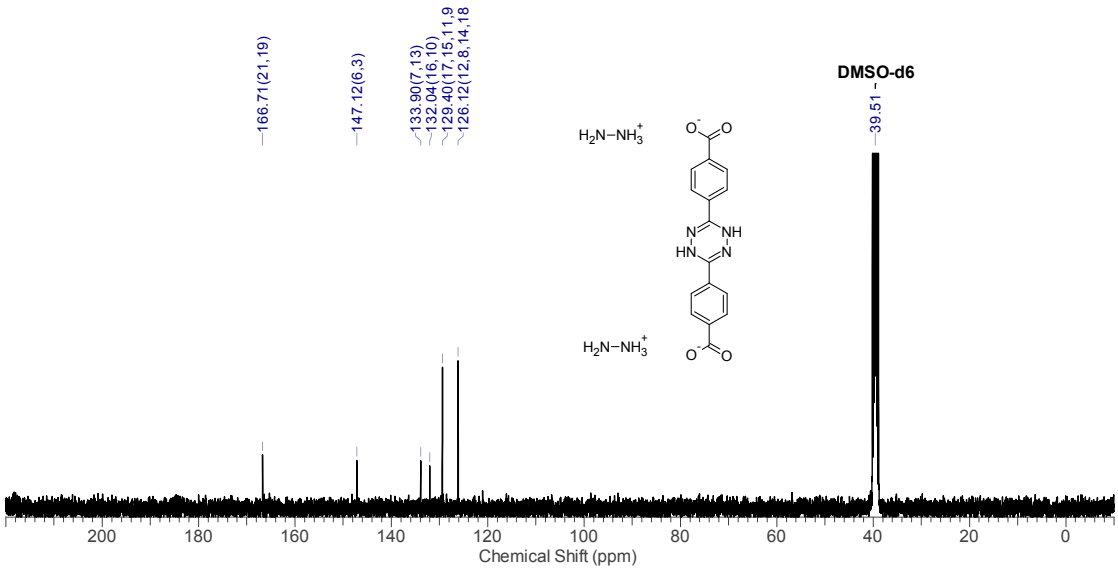


**Fig S7.** 13C NMR (101 MHz, DMSO-d6) of 4,4'-(1,2,4,5-tetrazine-3,6-diyl)dibenzoic.

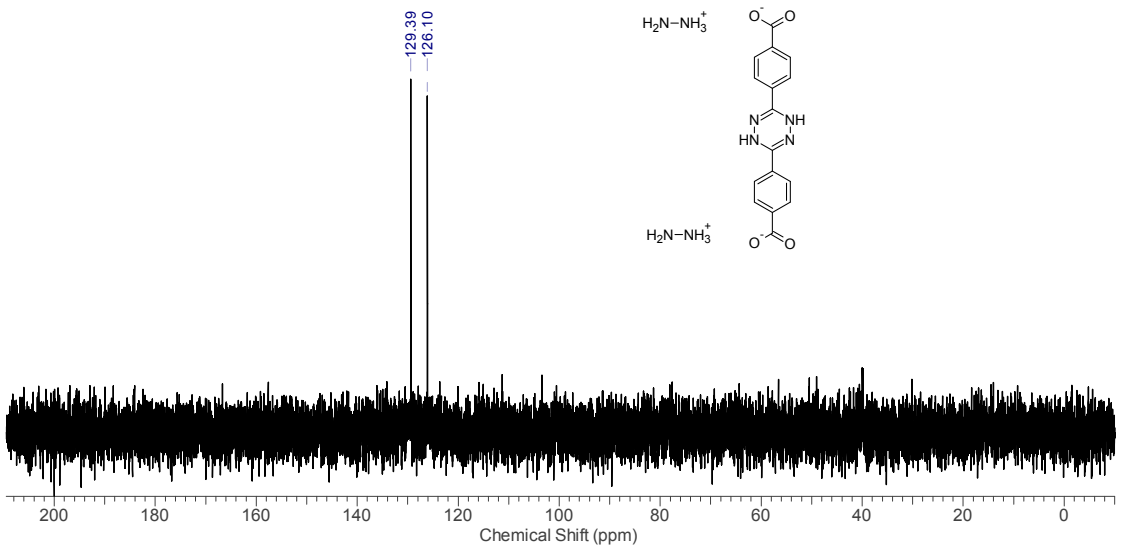


**Fig S8**. DEPT135 NMR (101 MHz, DMSO-d6) of 4,4'-(1,2,4,5-tetrazine-3,6-diyl)dibenzoic.

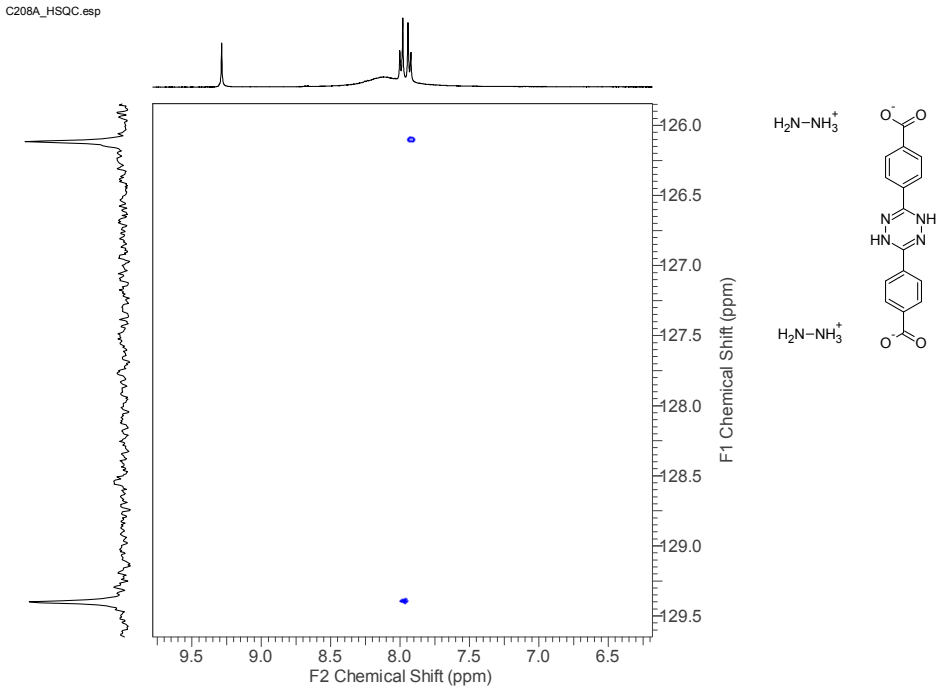


5 **Fig S9.** HSQC NMR (101 MHz, DMSO-d6) of 4,4'-(1,2,4,5-tetrazine-3,6-diyl)dibenzoic.

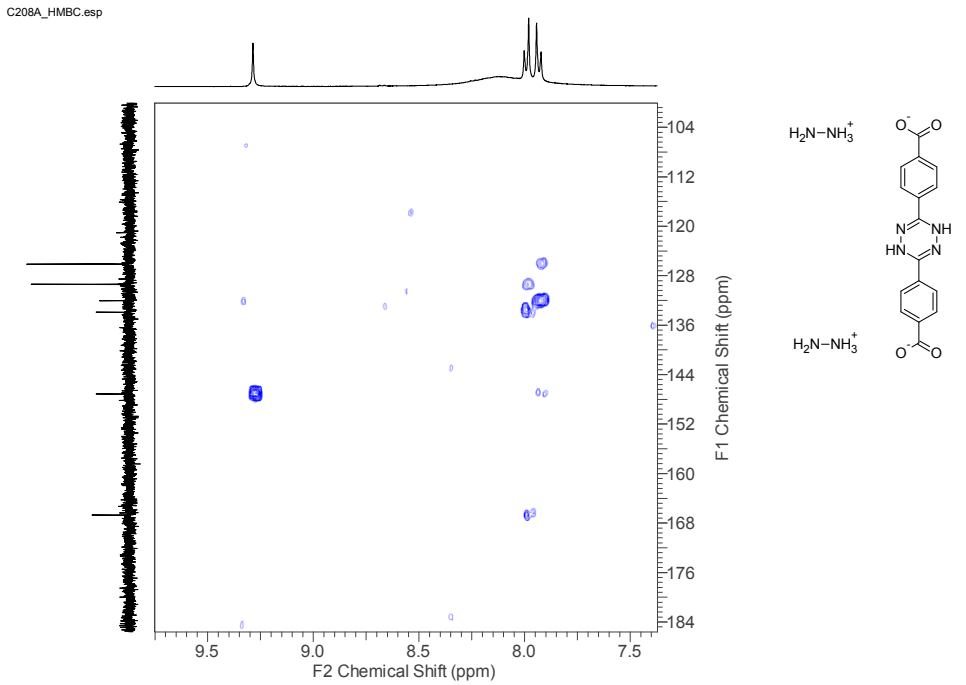


**Fig S10.** HMBC NMR (101 MHz, DMSO-d6) of 4,4'-(1,2,4,5-tetrazine-3,6-diyl)dibenzoic.

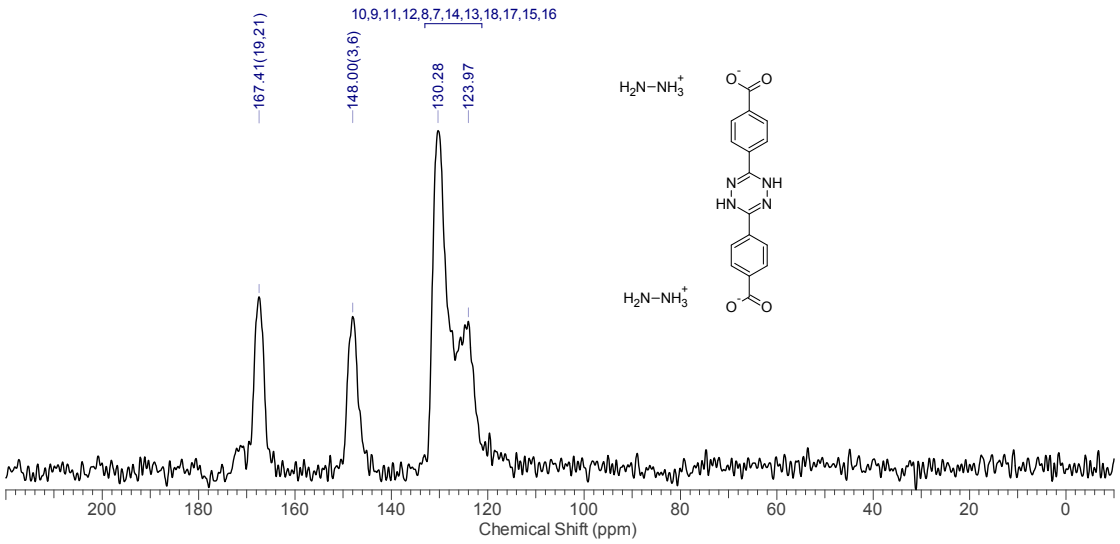


**Fig S11**. $^{13}C$ CP/MAS TOSS NMR spectra of 4,4'-(1,2,4,5-tetrazine-3,6-diyl)dibenzoic.

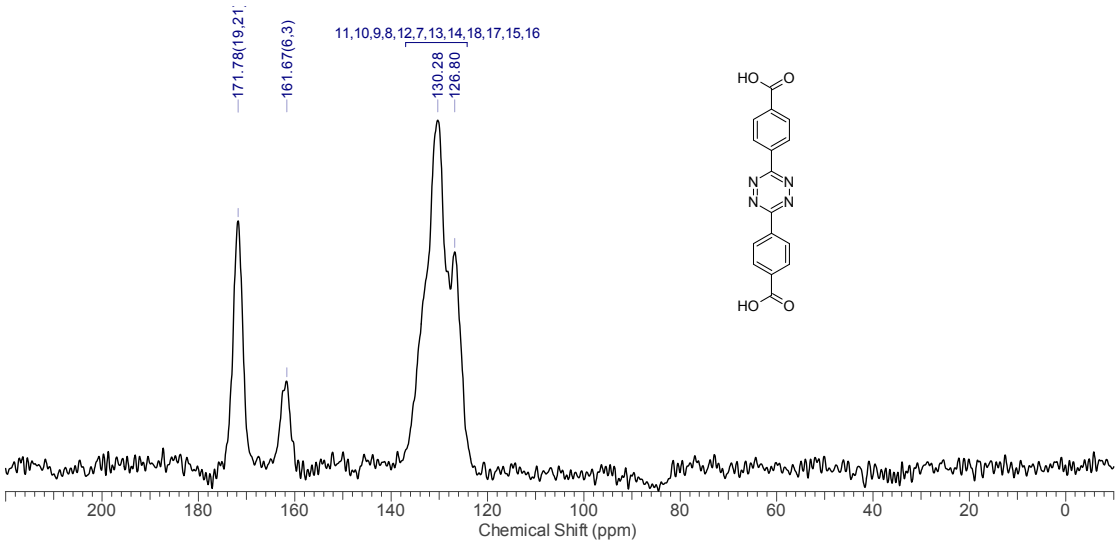


**Fig S12.** $^{13}$C CP/MAS TOSS NMR spectra of 4,4'-(1,2,4,5-tetrazine-3,6-diyl)dibenzoic.

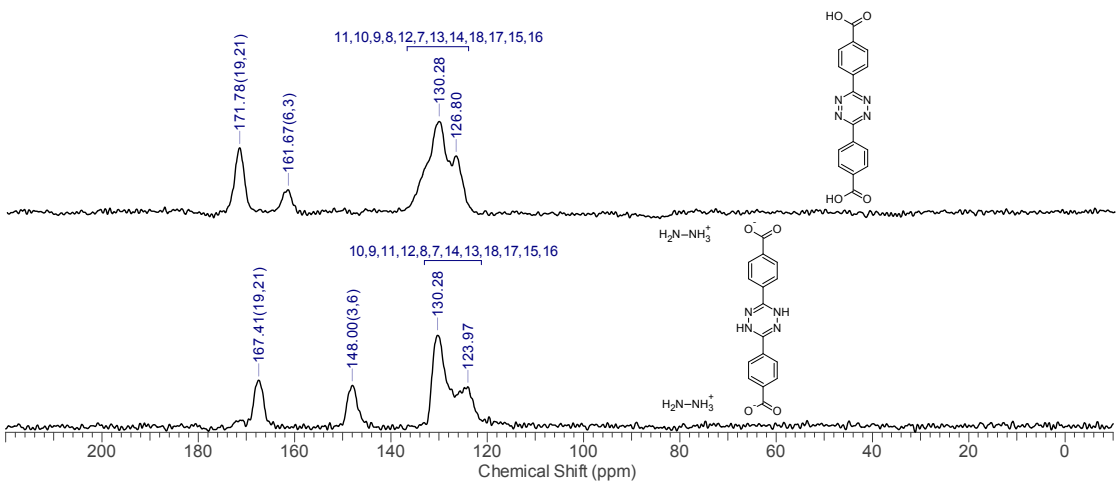


**Fig S13.** $^{13}$C CP/MAS TOSS NMR spectra comparation between precursor compound and **1**.

## References


1) G. M. Sheldrick, *SHELX97, program for crystal structure refinement*, University of Göttingen, Göttingen, Germany, 1997.

2) A. K. Rappé, C. J. Casewit, K. S. Colwell, W. A. Goddard and W. M. Skiff, *J.Am.Chem.Soc*. 1992, **114**, 10024.

3) A. K. Rappé and Goddard III, W. A. *J.Phys.Chem*., 1991, 3358.

4) D. Frenkel, B. Smit, Understanding Molecular Simulations: From Algorithms to Applications. 2nd ed.; Academic Press: San Diego, 2002.

5) D. Dubbeldam, S. Calero, D. E. Ellis, R. Q. Snurr, RASPA 1.0; Northwestern University: Evanston, IL, 2008.

6) R. C. Reid, J. M. Pausnitz, B. E. Poling, The properties of gases & liquids. 4th ed.; McGraw-Hill Companies: New York, 1987.